IOP Conf. Series: Materials Science and Engineering **1344** (2026) 012060 doi:10.1088/1757-899X/1344/1/012060

Development of the 17-kW orifice-type heater control system for thermal compensation induced by nuclear heating at the ESS hydrogen moderators

A Horvath[1*], H Tatsumoto[1] and T Vasilopoulos[1]

[1] European Spallation Source (ESS) ERIC, Lund, Sweden

[*]E-mail: attila.horvath@ess.eu

Abstract. At the European Spallation Source (ESS), a high-power, fast-response heater was developed to maintain stable operation of the Cryogenic Moderator System (CMS) by compensating for the 17kW of nuclear heating at the moderators when the 5 MW proton beam is switched on or off. The heater consists of 15 individual sheathed elements submerged in liquid hydrogen. For power regulation, a commercially available industrial 230VAC TRIAC-based control system was selected, offering a reliable and cost-efficient solution. Within the CMS Process Control System (PCS), a dedicated device type was implemented to manage all heater elements as a single unit, ensuring uniform power distribution and achieving an output power accuracy better than approximately 17W with a response time of under 10ms. This paper presents the electrical and software design, implementation details, and preliminary test results of the 17kW orifice-type heater control system.

1. Introduction

The European Spallation Source ERIC (ESS) is one of the largest science and technology infrastructure project being built in Sweden [1]. Protons at 2 GeV (with a normal current of 62.5 mA) are delivered by a superconducting linear proton accelerator and are injected onto a rotating tungsten target at a pulsed repetition rate of 14 Hz. Neutrons via spallation reaction are moderated to cold and thermal energies by two dedicated moderators as shown in Fig. 1, The cryogenic moderator system (CMS) was designed to circulate subcooled liquid hydrogen at a temperature of 17 K and a pressure of 1.0 MPa to remove static and dynamic heat load induced by the nuclear heating at the moderators, which is estimated to be 6.7 kW for a 5-MW proton beam power, increasing to 17.2 kW for the four-moderator configuration in the future. The CMS is cooled via a plate-fin type heat exchanger by a large-scale 20 K helium refrigeration system, referred to as the Target Moderator Cryoplant (TMCP) with a cooling capacity of 30.3 kW at 15 K. To compensate for transient heat loads applied to the CMS induced by the nuclear heating of the moderators, a 17kW orifice type electrical heater installed within the CMS loop after the moderators. With its high-power heating output and fast response time it is essential to enhance the stability of the CMS and TMCP by ensuring that the heat load transferred from the CMS to the TMCP remains constant.

The heating system mechanical design as seen on Fig. 2 consists of four parts: a heater insert where all the individual electrical heaters are located, a heater vessel, a vacuum vessel and an electrical enclosure providing explosion protection. The system's maximum total heating power

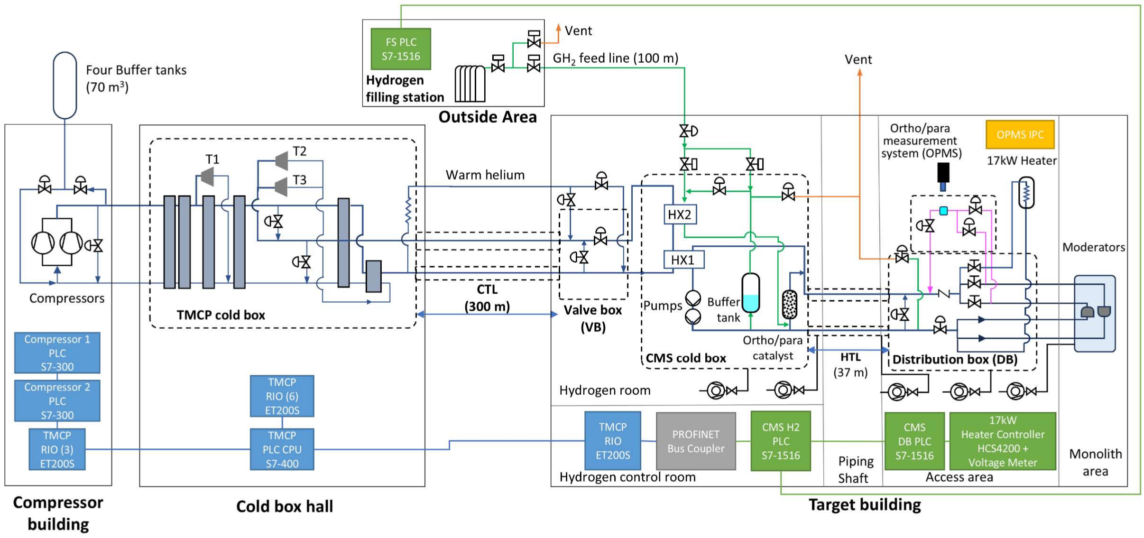

Figure 1. Overview of the cryogenic moderator system (CMS) process and control system.

is 18.7 kW, which includes a 10% margin. The heater consists of 15 individual sheathed heating elements submerged in liquid hydrogen, enabling rapid process response. This configuration keeps the surface temperature of the elements below 29 K and enhances the precision of the total heater power output, as detailed further below.

As shown in Fig. 1, The CMS PCS is a distributed control system based on multiple Programmable Logic Controllers (PLCs) and is responsible of controlling a wide array of equipment, consequently the system logic was designed with modularity, ease of expansion, and maintainability in mind [3]. The main PLC located in the hydrogen control room contains the process logic and controls all the field devices in its proximity, a second PLC located in the access area controls all the devices in its proximity including the 17kW heater as well, while the third PLC is responsible for the process logic of the hydrogen filling station. An isolated network provides the connection between the various PLCs and field devices minimizing the effects of any external disturbances. Different device types are implemented using custom software control blocks providing a wide range of features and Operator Interface (OPI) block icons and faceplates.

This study presents the electrical and software design, along with the implementation and integration details of the heater control system, as well as preliminary test results in helium.

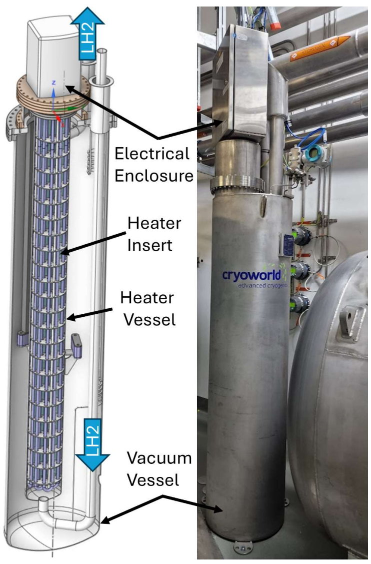

Figure 2. 17kW Heater.

IOP Conf. Series: Materials Science and Engineering **1344** (2026) 012060 doi:10.1088/1757-899X/1344/1/012060

2. Heater Electrical Design

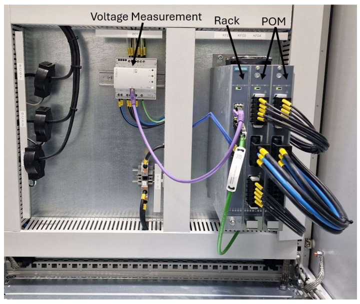

Figure 3. Heater Controller in the automation cabinet

The electrical design of the heating system depends on the chosen control method, which can be based on either Direct Current (DC) or Alternating Current (AC) power. Although DC power allows for smooth operation and high-power accuracy, it requires additional conversion from the more commonly available AC power, making it a less cost-effective option. Meanwhile, in AC-powered systems, the desired power output is typically achieved by cycling the heater On and Off. The switching frequency significantly influences the control precision. Low switching frequencies, typically implemented using mechanical devices like contactors, provide basic On-Off control by fully energizing or de-energizing the heater. In contrast, higher switching frequencies achieved using solid-state devices such as thyristors allow for finer control and improved power accuracy. Given these advantages, the high-frequency, solid-state switching method was selected for this application. Important to mention that the mechanical design of the heater total power of 17.2kW to be distributed across 15 elements was not only beneficial from the process point of view ensuring the desired low heater surface temperatures but enables “step control” where we can further increase the power accuracy by decreasing the minimum power step that is achievable as detailed below.

Another important consideration was the ease of integration into the existing SIEMENS PLC-based PCS. A common integration method for any field device is using Analog Input (AI) and Analog Output (AO) 4-20mA channels. This method is relatively simple, however considering the number of heater elements the PLC rack would have required additional Input and Output (IO) cards to be installed to the PLC rack, furthermore if these signals drift slightly from the off current level (usually 4mA) they can never be deenergized completely unless paired with digital On-Off control usually implemented via contactors.

With all the above considerations to be met a heater controller (HC) that uses AC voltage-based control and is widely used in industrial heating application (ex. Furnace control) manufactured from SIEMENS was selected from the SIPLUS HCS product family as seen on Fig. 3. Given that it’s manufactured by the same company as the components utilized in the PCS it allows for easy integration using the PROFINET protocol. The use of a fieldbus protocol eliminated the need for expanding the PLC rack, and the use of hardwired AI and AO based connections.

The HC can be customized depending on the size of the application by different rack sizes and Power Module (POM) combinations. In this application a compact rack is used where two identical POMs are connected. One POM can provide a total of 12 individually addressable and controllable heating elements as seen on Fig. 4. Each output can deliver a maximum of 3680W at 230VAC with a maximum power capacity of 29.4kW / POM and is based on TRIAC control. The heater elements were selected with this constraint in mind setting the heating element supply voltage of 230VAC, 50Hz where 15 elements together can provide a total power output of ~18kW depending on the electrical grid voltage.

To ensure overtemperature protection a T-type thermocouple is mounted on the surface of one of the heaters providing surface temperature measurement. The thermocouple is connected to a transmitter converting the signal to 4-20mA this later is split where one channel is connected to the PLC Analog Input and another one to a universal trip amplifier. The amplifier provides a

24 VDC signal to a PLC Digital Output, which can energize the contactor. This setup ensures the PLC can de-energize the POMs, while also provides independent and redundant overtemperature

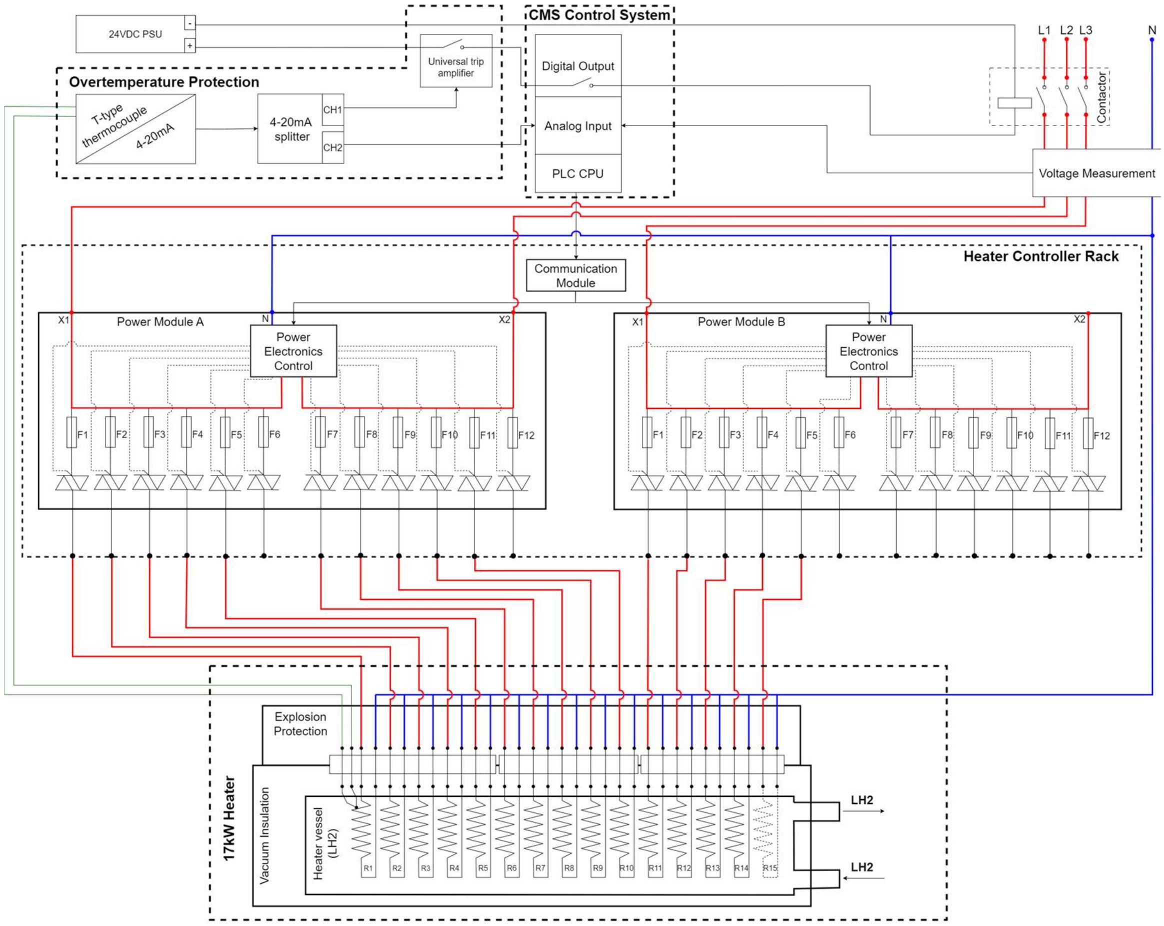

Figure 4. Simplified electrical and logical diagram of the heater controller.

protection from the trip amplifier that is configured to break the circuit if the heater surface temperature exceeds 50 °C as seen on Fig. 4.

Additionally, to compensate for the missing functionalities of the HC, a fieldbus-connected voltage measurement unit was included to monitor each line voltage individually. Based on the functionalities provided by these components, the heater control logic was developed to address these shortcomings, as further described below.

3. Heater Control Logic

3.1 Control System Integration

As shown in Fig. 5, to provide intuitive operation and comprehensive control, a new device type was developed in the PCS with a custom Operator Interface (OPI) Faceplate and a dedicated block icon. At the core, this software block ensures the integration of the HC into the PCS, primarily through cyclic data exchange. This exchange supports essential commands such as setting power setpoints and toggling global heating On or Off. When the global heating is turned Off via this interface, the HC sets all the setpoints to 0% and ignores any incoming setpoint commands,

IOP Conf. Series: Materials Science and Engineering **1344** (2026) 012060 doi:10.1088/1757-899X/1344/1/012060

effectively stopping all heater outputs. It is important to note while the outcome of this is similar to the deenergized contactor this functionality is just a software one so it can't replace the mechanical disconnection of the power. In addition to basic control, more advanced diagnostics such as broken loop detection are handled through acyclic, event-driven signal exchange. This mechanism allows the HC to report hardware-level faults or irregularities to the PCS promptly, enabling timely operator response or automatic intervention.

3.2 Heater Power Distribution

Each POM channel in this application receives integer setpoints expressed as percentages in engineering units. These output channels operate in "Half-wave" control mode, where a 100% setpoint corresponds to applying the full 50Hz grid voltage waveform to the heater element. This control mode is heavily affected by power grid disturbances that are limited on the Swedish network to +/-10% above and below the 230VAC nominal level for every 10-minute mean value. These disturbances affect the repeatability and the stability of the heater power output. To compensate for this the implemented software block accepts the combined global setpoint $P_{Setpoint}$ in watts represented as a real. By utilizing the known resistance and real-time line voltage of each individual heating element, the software block dynamically calculates the setpoints for each output channel to achieve the desired total power. At the same time, it ensures a balanced power distribution across all elements, as illustrated below:

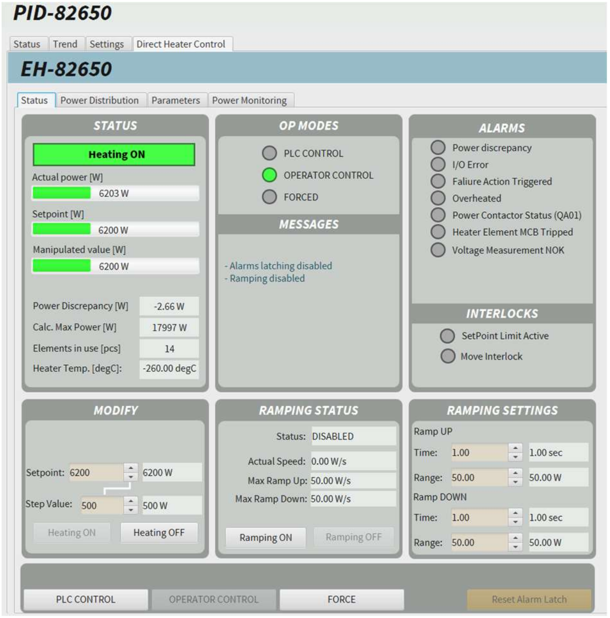

Figure 5. Operator Interface

$$P_{total} = \sum_{i=1}^{n} P_{base\_i} + P_{fine} \tag{1}$$

Where n is the total number of configured and in use elements; i and j are the heater element indexes; V is the line voltage and R is the resistance of the heater element.

$$P_{base\_i} = \frac{P_{Setpoint} - \sum_{j=1}^{i-1}\left(\frac{P_{base\_j\_SP} * V_j^2}{100 * R_j}\right)}{n - i} \tag{2}$$

$$P_{base\_i\_SP} = \left\lfloor \frac{100 * R_i * P_{base\_i}}{V_i^2} \right\rfloor \tag{3}$$

The above calculation to determine the base setpoint in percentage for every heater element is calculated every PLC CPU cycle and propagated to the PROFINET IO-System of the HC ensuring the response time for the $P_{base\_i\_SP}$ to be comparable with the cycle time of the PLC CPU of approximately 10ms. In addition to balancing power distribution across the elements, this algorithm compensates for variations in supply voltage and manufacturing tolerances between the heater elements, whose resistance values were measured to range from 39.7 Ω to 46.9 Ω. It also ensures that the maximum base power error (that P_{fine} shall compensate) remains below the smallest achievable power increment of the final heater element receiving a setpoint. Even under the worst-case conditions (i.e., lowest heater resistance and highest supply voltage) this error remains below 16.12 W which corresponds to a hydrogen temperature variation of 0.01K at 10bara, 17.5K and a mass flow of 0.25kg/s:

$$P_{base\_error} < \frac{V_n^2}{100 * R_n} \tag{4}$$

Where V_n, R_n are the supply voltage and the resistance of the final heater element to receive the setpoint. To compensate for this error the P_{fine_SP} is calculated as seen below:

$$P_{fine\_SP} = \begin{cases} +1\%, & if \ \frac{1}{\tau}\int_{t=-\tau}^{t=0} P_{error}(t)dt < 0 \\ -1\%, & if \ \frac{1}{\tau}\int_{t=-\tau}^{t=0} P_{error}(t)dt > 0 \end{cases} \tag{5}$$

Where if $P_{fine\_SP} = +1$ then it is applied to the currently lowest base power output heater, else if $P_{fine\_SP} = -1$ is subtracted from the highest base power output heater, τ is the rolling buffer time for the average error calculation. The selection of τ will affect the overall system response time but is heavily dependent on the electrical installation at hand. In this application it was defined to be a total of 100 PLC CPU cycles (~1000ms). The P_{error} can be calculated as:

$$P_{error} = P_{Setpoint} - P_{total} \tag{6}$$

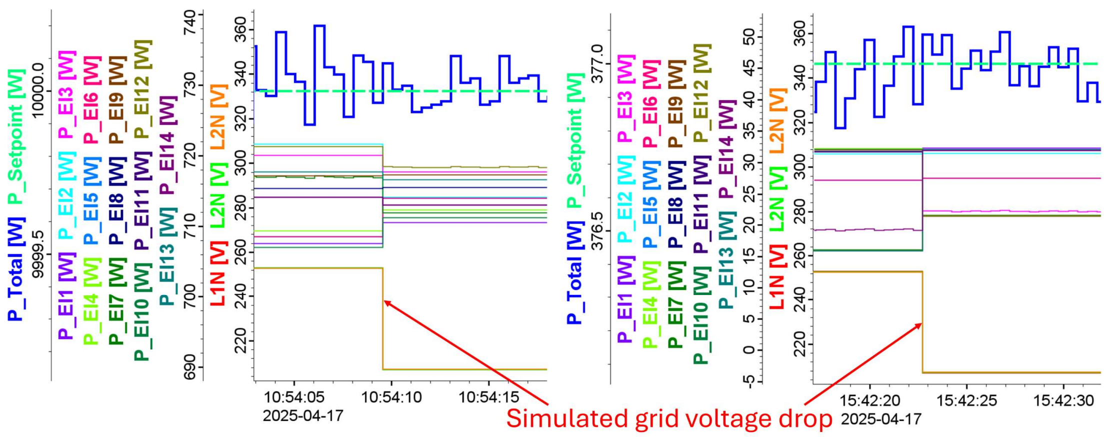

Figure 6. Power output response to simulated grid voltage variations in low and high-power scenarios output situations

Fig. 6 illustrates the simulation results of power grid disturbances, demonstrating the response of the power distribution control logic to step-type fluctuations in grid voltage within the permissible range of ±10% relative to the nominal 230 VAC. The results are presented for both low and high-power output scenarios. Even though such abrupt step changes in grid voltage are not representative of real-world conditions, as actual grid fluctuations tend to be significantly more gradual and moderate in nature it can be observed that the total power remained unaffected.

Health monitoring is also implemented, monitoring for configured but non-functional (broken) heater elements, for loss of phase power or voltage measurement. In this case the number of configured elements is updated in function of the number of the faulty elements (n_{faulty}):

$$n = n - n_{faulty} \tag{7}$$

Fig. 7 illustrates the system's response to a heater element failure where the total power output remains unaffected, as the remaining operational heater elements automatically compensated for the loss by increasing their power contribution.

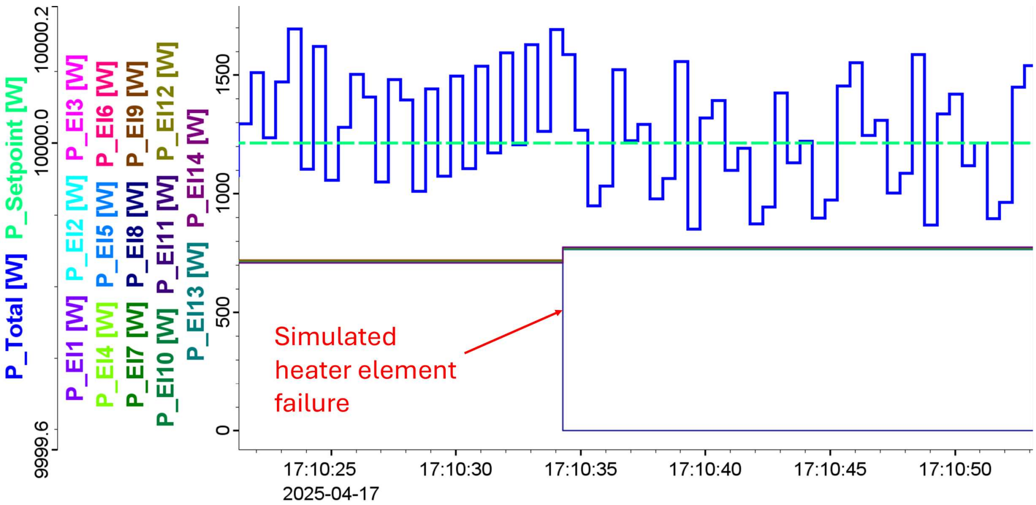

Figure 7. Simulated heater element failure

Other noteworthy functionalities are setpoint ramping, overheating protection that is configured to shut down all the heater elements earlier than the hardwired overheating protection, various alarming functionalities (ex. high power output discrepancy) and PID control algorithm allowing to control the return temperatures of the system in two different locations.

4. Initial test results

On Fig. 8 the tracking of the setpoint to the total power output and the error between them can be observed. The basic functions of the electrical heater together with its controller hardware and software functionalities were successfully tested during the preliminary CMS commissioning using helium at 17K prior to hydrogen operation with a total maximum of 500W. During these

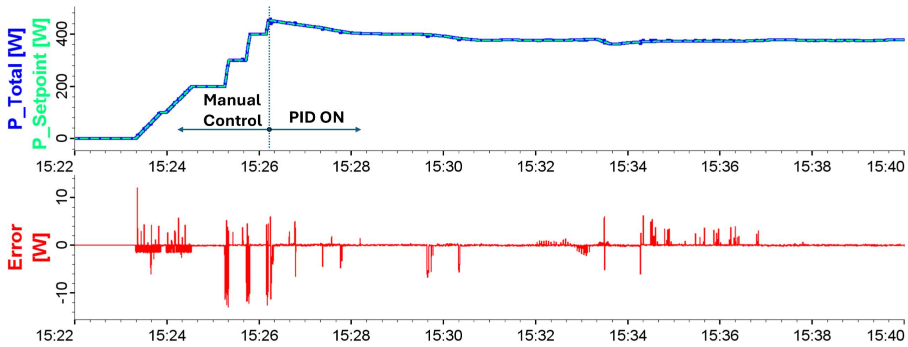

Figure 8. Total power output and system accuracy

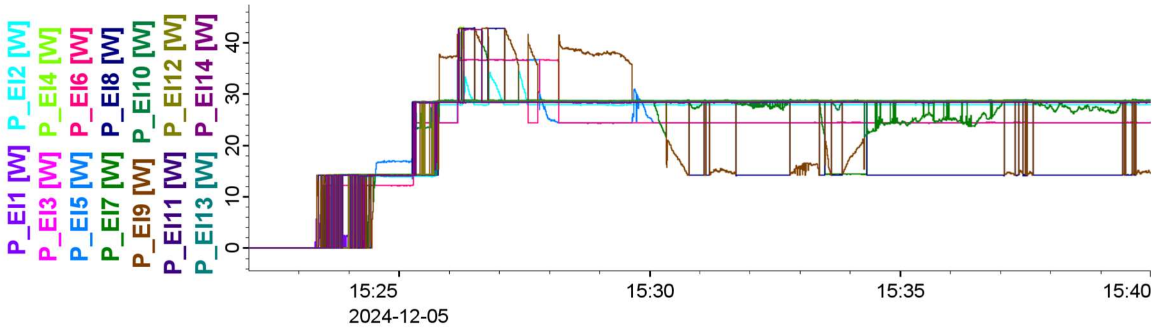

Figure 9. Power distribution across 14 heater elements

tests various ramping and step response of the heating system were tested together with the implemented Proportional Integrative and Derivative (PID) controller controlling the return temperature towards the CMS CBX.

Fig. 9 the power distribution between the heater elements. It was observed that during steep output power ramping tests, error spikes were more frequent, though they remained short in duration. Despite these transient deviations, the average error value remained close to zero.

The accuracy of the power output calculated by the PCS was evaluated by comparing it to power estimates derived from energy balance calculations. The results of this comparison are presented Fig. 10.

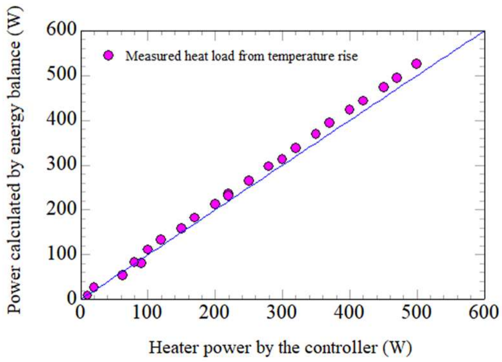

Figure 10. Calculated heater output power compared to calculated power based on energy balance

5. Conclusions

We developed a robust, high-accuracy, and cost-effective control system for the 17kW heater, fully integrated into the CMS PCS. Custom software logic and OPI elements were implemented to provide essential functionalities such as balanced power distribution, compensation for resistance variations and grid voltage fluctuations, fault detection, overtemperature protection, setpoint ramping, and PID control. These features were successfully validated with a maximum of 500W power output during CMS commissioning activities with helium, demonstrating reliable performance and confirming the system's readiness for hydrogen commissioning at higher power levels.

References

[1] Garoby R and Danared H et al 2018 *Phys. Scr.* **93** 014001
[2] Tatsumoto H, Horvath A and P Arnold "Basic design of a 17-kW orifice type heater for the ESS cryogenic moderator system", presented in CEC-ICMC 2025 (C2Po1A-06), submitted to *Adv. in Cry. Eng.* (at press)
[3] A Horváth, M Boros, Tatsumoto H and T Vasilopoulos 2025 *IOP Conf. Ser.: Mater. Sci. Eng.* **1327** 012164